WCTE 2016
World Conference on Timber Engineering
August 22-25, 2016 | Vienna, Austria

THE DESIGN OF CROSS-LAMINATED TIMBER SLABS WITH CUT-BACK GLULAM RIB DOWNSTANDS – FROM RESEARCH TO LIVE PROJECT

Panayiotis Papastavrou[1], Simon Smith[2], Tristan Wallwork[3], Allan McRobie[4], Nicholas Niem[5]

ABSTRACT: A research project was undertaken to investigate the behaviour of composite CLT slabs with glulam downstands cut back from the supports. A desk study and Finite Element Modelling (FEM) were used and evaluated on their ability to model and design such a structure, focusing on the cut back location and utilising reinforcement screws. The project included full-scale laboratory testing of a composite slab to failure with innovative data collection techniques such as Particle Image Velocimetry. A similar structural element was also used in a real construction project and the investigation gave insight towards its design. It was concluded that the embedment depth of reinforcement screws in the glulam downstand is key to the performance of the composite slab with full depth penetration advisable. FEM can give useful results for stress concentrations in the timber and a simplified design method was proposed.

KEYWORDS: Cross-Laminated Timber, Composite Slabs, Particle Image Velocimetry, Finite Element Modelling

1 INTRODUCTION

A research project was undertaken at the University of Cambridge to investigate the behaviour of composite slabs with a CLT deck and glulam downstands. Particular focus was given on the design scenario of stopping the downstand beam short of the support and its effect on localised stresses in the area.
The project included finite element modelling and full scale lab testing as well as being implemented on a live construction project that is now complete.

2 CLT RIBBED SLABS

2.1 MOTIVATION

Cross-Laminated Timber floor panels are typically used for spans up to 7-8m under relatively lightweight floor build-up in office/classroom usage class. For these spans, the floor thickness required is approximately 250-300mm and the governing factors are serviceability limit states (SLS) to Eurocode design with the most common limiting criteria being vibration characteristics.
A backspan could be utilised to enhance the deflection performance and this being unequal to the main span would slightly enhance the vibration performance as well. However, this means that single floor panels need to be increased in length to beyond 8m which might start to introduce other issues in terms of transport costs and access restrictions. It should be noted that, normally, CLT floor panels are limited by manufacturers to 13.5m lengths.
An alternative way to provide the additional stiffness required to meet the SLS criteria is to install Glulam downstand ribs to the underside of the floor panel. The structural element is then a "CLT Ribbed Slab". Gluing technology during fabrication allows the ribbed slab to be manufactured with a fully-composite connection between slab and ribs which can be utilised in the design.

2.2 STRUCTURAL DESIGN

The design of fully-composite CLT ribbed slabs has been the subject of some publications to date and references are included here for completeness.
As per the design of T-beams in other more conventional materials e.g. reinforced concrete, the concept of the effective slab width, b_{ef}, needs to be considered as a result of shear lag. This is introduced for CLT ribbed slabs in [1] and provides an approximate reduced slab width to be used when calculating the design stresses and deflections due to the non-uniform normal stresses in the slab. See Figure 1 and Figure 2 below.

[1] Panayiotis Papastavrou, Smith and Wallwork Engineers, Cambridge, UK, panayiotis.papastavrou@smithandwallwork.com
[2] Simon Smith, Smith and Wallwork Engineers, Cambridge, UK, simon.smith@smithandwallwork.com
[3] Tristan Wallwork, Smith and Wallwork Engineers, Cambridge, UK, tristan.wallwork@smithandwallwork.com
[4] Allan McRobie, Cambridge University Engineering Department, Cambridge, UK, fam@eng.cam.ac.uk
[5] Nicholas Niem, Ramboll UK, London, UK, nicholasniem@outlook.com

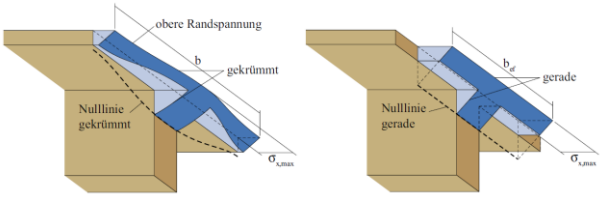

Figure 1: *Actual (left) and approximated (right) normal stress distributions showing effective width concept* **[1]**

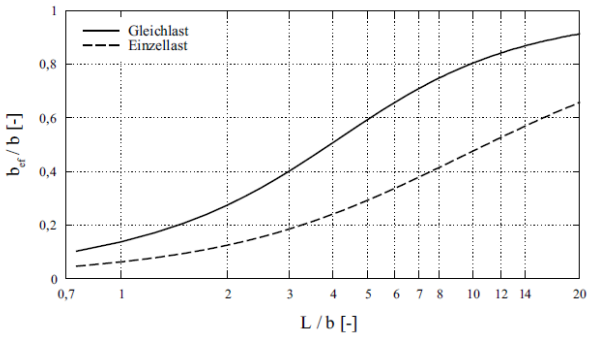

Figure 2: *Effective width design chart for CLT ribbed slabs-top curve for mid-span, bottom curve for support calculations* **[1]**

Furthermore, the effective widths calculated from the methods noted above are used to obtain the flexural stiffness of the cross-section, $(EI)_{eff}$. There are various methods to calculate this including the Gamma-method, the K-method and the ShearAnalogy method. As suggested in [2], the ShearAnalogy method seems to be the most accurate and has been adopted in this research paper as shown in Equation (1) below.

$$(EI)_{eff} = \sum_{i=1}^{n}\left(E_i \frac{b_i t_i^3}{12} + E_i A_i z_i^2\right) \qquad (1)$$

where E_i = Young's modulus of layer i, A_i = Area of layer i and remaining properties as Figure 3 below.

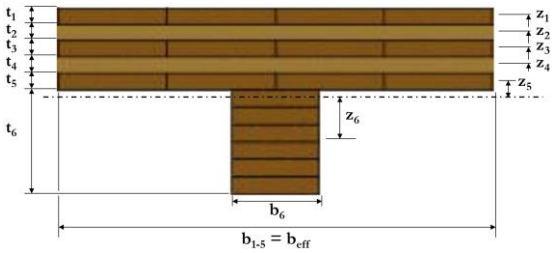

Figure 3: *$(EI)_{eff}$ calculation parameters*

Stresses for Ultimate Limit States (ULS) calculations are calculated using the equations below [3], for normal stress, σ, (Equation 2) and shear stress, τ, (Equation 3):

$$\sigma(z) = \frac{M.E(z).z}{(EI)_{eff}} \qquad (2)$$

$$\tau(z) = \frac{S \int E(z).z\, dA}{(EI)_{eff}.b_{cut}} \qquad (3)$$

where M = applied moment, S = applied shear force, E(z) = Young's modulus of layer at depth z from the neutral axis, b_{cut} = width of shear surface obtained from Figure 4 below.

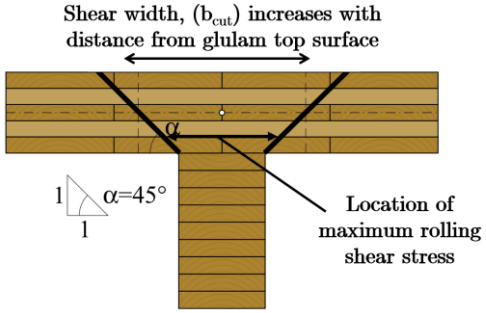

Figure 4: *Shear width within a CLT-glulam section* **[1]**

For SLS checks, the deflections can be calculated by allowing for both the flexural and shear deflections. The flexural deflections can be approximated using Timoshenko beam theory and $(EI)_{eff}$ obtained above, however, the shear deflections for CLT ribbed slabs are more complicated to calculate and reference should be made to the research report for background and more details [4].

Vibration checks based on the natural frequency of the ribbed slab can be carried out using:

$$f = \frac{\pi}{2L^2}\sqrt{\frac{(EI)_{eff}}{m}} \qquad (4)$$

where m = mass per unit length and L = span.

2.3 CUT-BACK RIBS

The following research is concerned with the design of ribbed slabs with the ribs cut back from the supports. This type of slab is of interest and use in the construction industry and the concept is illustrated in Figure 5 below.

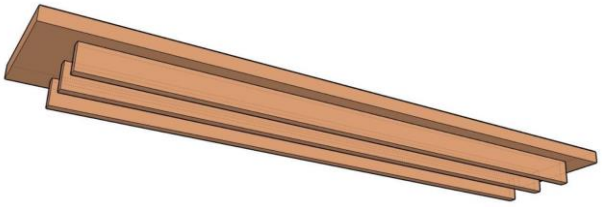

Figure 5: *CLT ribbed slab with cut-back glulam ribs (12m span with 0.5m cut-back shown)*

More often than not, the option to have flat soffits is preferable for the horizontal distribution of services. The introduction of deep downstands can disturb the service routes along the slab soffits and push them downwards. This can reduce the available floor-to-ceiling depths and also increases the complexity of the services. Cutting the ribs back from the support can allow the services to run straight through along the slab soffit at the support locations and this is illustrated in Figure 6 below.

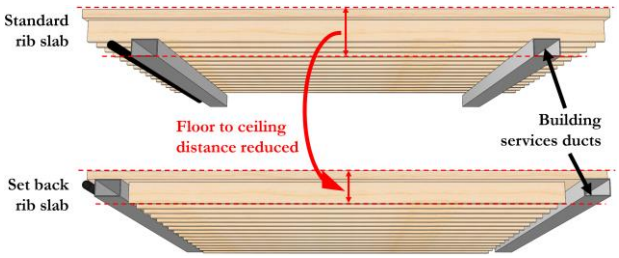

Figure 6: *Services interaction with CLT ribbed slab*

Additionally, not having the ribs continue to the supports makes the actual support construction very simple. As only the slab needs to have direct bearing, the support needs only be a flat surface which is the most common scenario in the platform construction method usually adopted for CLT structures. Otherwise, should support be required for the ribs, a castellated arrangement needs to be provided or complex shear connections at each rib location made to the supporting structure. This is illustrated in Figure 7 below.

Figure 7: *Non-preferable support conditions - castellated walls (left), shear connection (right). (credit KLH)*

3 RESEARCH PROJECT

A research project was undertaken at the Cambridge University Engineering Department to investigate the CLT ribbed slab system with cut-back ribs as a structural floor element.

The project tried to identify whether the use of Finite Element (FE) Modelling can be used to accurately predict the behaviour of complex CLT, glulam and screw systems, the effect of the cut-back on the performance and provide simple guidelines towards the design of such systems.

The investigation comprised of an initial desk study during which a CLT ribbed slab was modelled, analysed and designed to withstand a certain load, followed by full-scale testing of a 5.8mx2.4m 200mm thick CLT slab with three 140x500 glulam ribs.

Figure 8 below indicates the stress notation used in the project and referred to from this point forward.

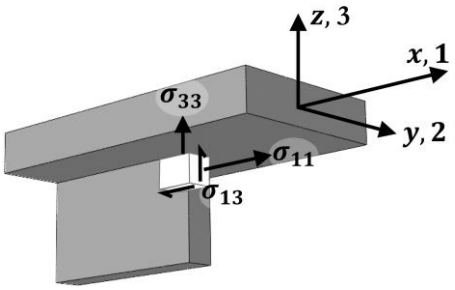

Figure 8: *Stress notations and directions*

3.1 DESIGN PROCESS – DESK STUDY

3.1.1 Analysis methods and validations

An Excel spreadsheet was developed that used all the already established research around CLT ribbed slabs explained in Section 2.2 above to produce theoretical predictions for stresses, deflections and vibration. These results would be used as the baseline of comparison of an FE model developed in the ABAQUS software package.

The use of FE modelling was one of the initial targets of the project, as computational flexibilities come at a lower cost than practical testing, and validation is always a basic requirement of such tools. Validation was done in several stages, starting with modelling a CLT slab on its own, allowing for the different material properties of the layers within the slab depth. Once this gave acceptable results, the ribs were added as well and a typical output from the FE model is shown in Figure 9 below.

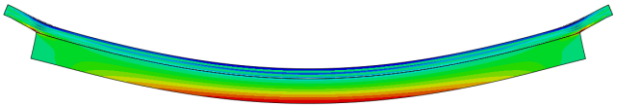

Figure 9: *Normal stresses and deflected shape of a simply-supported CLT ribbed slab with cut-back ribs (12m span and 9kPa UDL) – concentration of stresses in the CLT slab can be seen at the cut-back locations*

Figure 10 and Figure 11 below are extracts from some of the validation comparisons between the Excel spreadsheet results (Theoretical prediction) and the FE model (ABAQUS results).

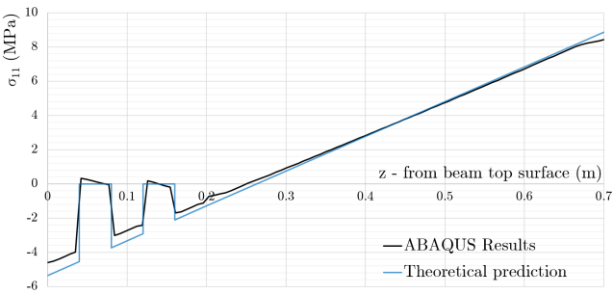

Figure 10: *Normal stresses along a vertical plane at mid-span of a simply-supported CLT ribbed slab with cut-back ribs (12m span and 9kPa UDL)*

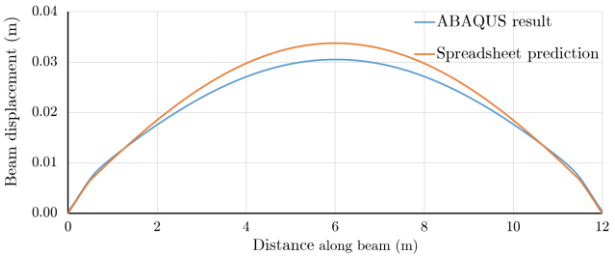

Figure 11: *Deflection of a CLT ribbed slab with cut-back ribs (12m span, 9kPa UDL)*

Some differences between the 2 methods were observed which were attributed to the likelihood that the effective widths used in the Excel are conservative, hence giving rise to higher stresses at the top of the slab (Figure 10) and lower flexural stiffness (higher deflections for spreadsheet prediction on Figure 11). Based on the validations, the FE model developed was deemed as capable of replicating the behaviour of the CLT ribbed slab and would be used moving forwards.

3.1.2 CLT Slab

After confidence was gained from the FE modelling, a set-up for a CLT ribbed slab with cut-back ribs was chosen to be designed and subsequently tested in the lab. This is shown in Figure 24 and formed the basis of the main FE model used.

From the FE modelling, and as seen in Figure 9, a concentration of normal stresses was observed at the cut back locations in the CLT slab. Due to the glulam rib not continuing to the support, the CLT slab beyond the rib is acting as a cantilever with a point load at the tip; the fixed end moment occurs at the end of the rib and the point load being the support reaction, P_f, as shown in Figure 12 below.

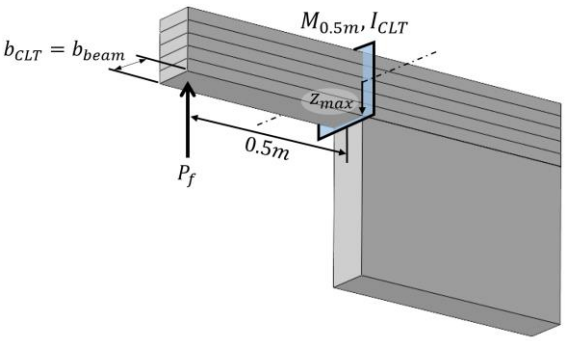

Figure 12: *Cantilever CLT slab design scenario at the location where the Glulam rib stops*

Using Equation (2) with the associated CLT slab properties, a limiting value for the support reaction, P_f, was calculated by inserting $M = P_f$ x 0.5m; the critical reaction was 40kN assuming that a constant width of CLT slab equal to the glulam rib width was active.

This gave an indication of when failure is expected in tension at the bottom layer and this load was carried forward for the remaining design checks. A 3-point bend set-up for the slab was derived with the central point load adjusted to provide the P_f calculated.

For completeness, the midspan moment capacity of the full T-section and the CLT slab-only rolling shear capacity at the support were checked that they were adequate under the design scenario of the 3-point bend test. This confirmed that the critical area of the ribbed slab was indeed at the cut-back location.

3.1.3 Rib cut-back location

An FE model with the above 3-point bend test scenario was developed to further investigate the stresses at the rib cut-back location. The CLT-to-glulam connection was taken as fully composite.

A check on the bending stresses estimated when calculating P_f above was undertaken by checking the tensile stresses in the CLT slab at the end of the rib given by the FE model. This is shown in Figure 13 below and can be seen that it is close to the relatively common bending strength of CLT slabs, $f_{m,k}$ = 24N/mm^2.

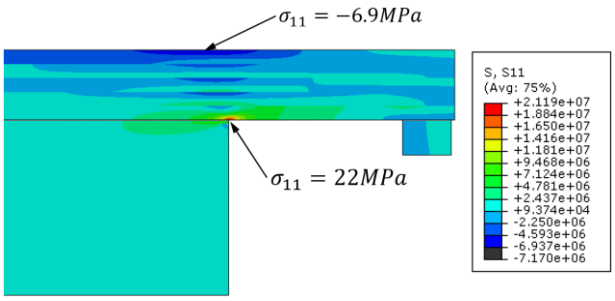

Figure 13: *Normal stress concentration in the CLT slab under 3-point bend test adopting the calculating support reaction, P_f*

The FE analysis concentrated at the end of the glulam rib as it was identified that the flow direction of the principal bending stresses will have to undergo a significant change in that location in order to cause the transition of the neutral axis from inside the rib to the middle of the slab (see Figure 14 below).

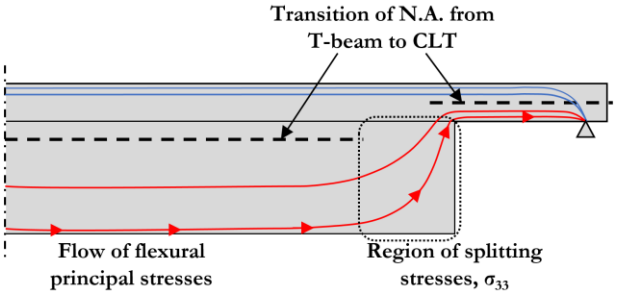

Figure 14: *Flow of principal stresses undergoes a change in direction at the rib cut-back location*

The change of the neutral axis vertically upwards suggests that the glulam rib end is a region with high stresses in the vertical direction i.e. stresses perpendicular to the grain of the rib. As this is a particularly weak direction in which to load a timber element and causes splitting, it was necessary to investigate the stresses in that direction, σ_{33}. The output from the FE model is shown in Figure 15 below.

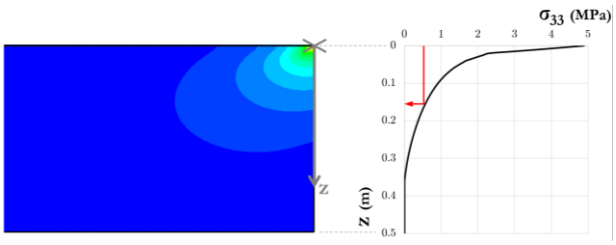

Figure 15: *Stress σ_{33} contours through the central plane of the glulam rib – right edge is the end of the rib at the cut-back location and the graph shows the variation of σ_{33} along that face with rib depth, z.*

High splitting stresses can be observed but BS EN 14080 suggests a value of just 0.5MPa for glulam GL28h tensile strength perpendicular to the grain. This was marked on the graph in Figure 15, and the depth in the glulam beyond which the stresses dropped to below that value was read off. A way to overcome the high splitting stresses was by the installation of fully threaded screws from the slab into the glulam rib, ensuring that they penetrate down to this depth to ensure that the timber does not split.

The σ_{33} stresses were seen to be of high magnitude up to a distance of 0.5m from the rib end. The total normal (V) and shear force (S) experienced by the CLT slab-glulam rib interface over that distance were calculated by numerical integration of σ_{33} and σ_{13} stresses respectively (see Figure 16 below). These forces were used to design the fully threaded screws to Eurocode 5 – V is the screw axial load to be carried and S the shear load.

Figure 16: Normal and shear forces used in the screw connection design

It was particularly interesting to observe that the integral of the tensile σ_{33} stresses (area under curve where σ_{33} is positive in Figure 17 below) produced a total force, V, higher than the support reaction, P_f. Moreover, the stresses σ_{33} became negative i.e. compressive, beyond the tensile region. This was thought to occur due to the moment that is present in the CLT slab at the glulam cut-back location which induces a couple via push-pull action at the CLT-glulam interface. The additional pull-out from the couple was then thought to increase the splitting force, V, beyond the apparent shear from the support reaction, P_f (V was found to be 55kN which is approximately 40% higher than P_f).

Subsequently, the FE model was developed even further to include the screws. To model the bond between the screw thread and the timber, a cylindrical element was introduced that was fixed to the timber using a tie constraint in ABAQUS.

The results from the updated analysis were of great interest as they showed that the effect of the screw did not particularly help as expected. Inserting the screw elements only partially into the glulam rib led to new high stress concentrations at the tip of the first pair of screws (see Figure 18 below).

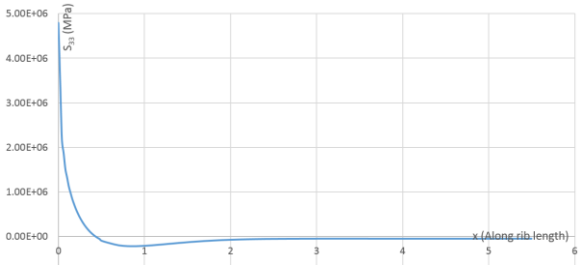

Figure 17: *Stresses σ33 along the CLT-glulam interface (x=0 at the glulam end)*

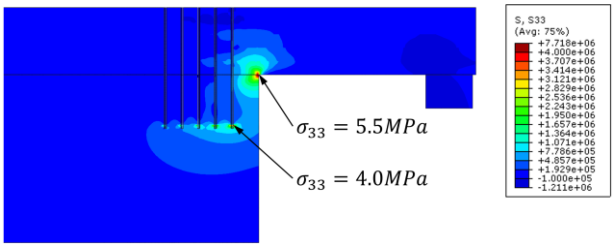

Figure 18: *FE model including screws showing σ_{33} stress concentration at the screw tips*

This σ_{33} stress was again much higher than the tensile timber strength perpendicular to the grain according to the Eurocode. The screw depth was varied in the FE model to investigate its effect and whether reaching the 0.5MPa strength suggested by the Eurocode is possible. The stress concentration relocated at the screw tips at every iteration but reduced in magnitude as shown in Figure 19 below. Even at double the initial depth, the stress did not drop below 1.5MPa.

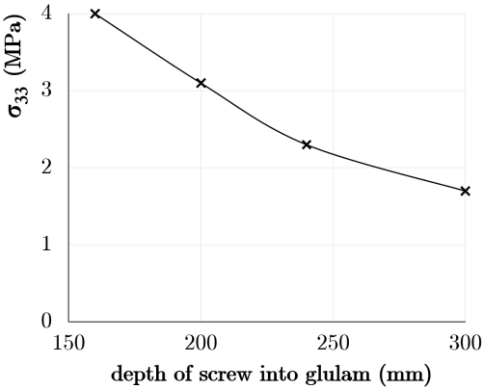

Figure 19: *Peak σ_{33} at screw tip for different lengths of screw i.e. penetrating deeper into the glulam rib*

Concluding the desk study, it was deduced that the weak point of such a set-up was at the screw tips where the tensile stress perpendicular to the grain is higher than the quoted strength of the relevant glulam standard.

The test sample that was to be tested was ordered before the final FE model that included the screws was developed. Thus, the screws inserted into the slab only penetrated the glulam rib by 160mm as suggested by the

first FE model. It was therefore predicted that the failure of the slab would occur before the full load required to yield a support reaction of P_f was reached due to the screw tip being already over-stressed by that point.

3.2 LABORATORY TESTING

3.2.1 Particle Image Velocimetry (PIV)

As described above, the stresses at the rib cut-back location play a significant role in the performance of the slab and, therefore, it was important to obtain some test data for these. The FE modelling yields contour plots of the stresses but common gauges and instrumentation cannot be used to replicate such detail in a real test.

Therefore, the Particle Image Velocimetry (PIV) technique was trialled. This method works by analysing successive high resolution images of a deforming textured surface. The analysis of the images described below is carried out in mathematical modelling software such as Matlab which was used for this project.

Each image is split into a grid formed by patches of pixels. The original image's patches are then tracked in the successive images taken as the surface is deforming. The tracking is done via a search patch which uses correlation functions to give a peak when the displaced location of the patch is found (see Figure 20 below). The displaced locations for all initial patches are then combined to generate a displacement field. Further analysis of this field can be done to yield the strain and stress fields.

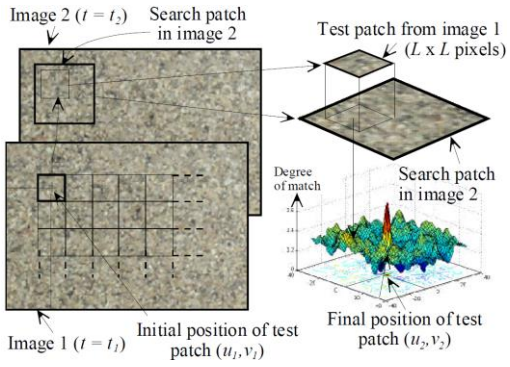

Figure 20: *PIV process*

The PIV technique and associated Matlab code had been used previously in the geotechnical engineering field but these were found unable to produce useful results for the stresses generated in a general beam bending scenario. The two main issues encountered is that the existing code could only generate volumetric and shear strains and that the pixel patches required to obtain recognisable patterns in the results were too big, smearing the results. Moreover, the numerical code was prone to "peak locking", an artefact of the sub-pixel resolution that leads to spurious strain fields (see Figure 23).

Therefore, in order to be able to use the PIV technique in the CLT ribbed slab project, new Matlab code was written that was capable of generating strain fields to sub-pixel accuracy using much smaller pixel patches at a shorter computational processing time.

The newly developed code was validated in a 3-point bend test of an aluminium box against a strain gauge. The set-up at mid-span is shown in Figure 21 below.

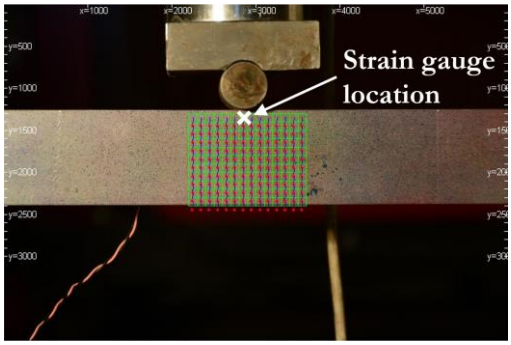

Figure 21: *Grid of pixels generated by PIV analysis under central point load in 3-point bend test of an aluminium box*

The horizontal strains at mid-span obtained from the 3-point test were compared between the new Matlab code (see Figure 22 below) and the existing geotechnical code (see Figure 23 below).

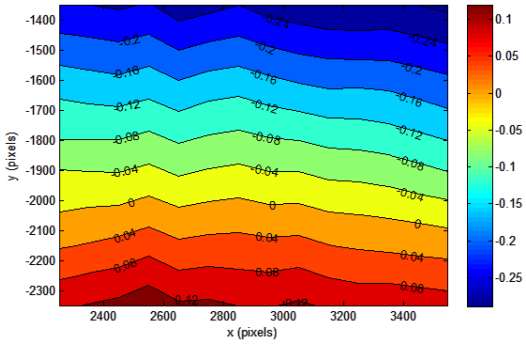

Figure 22: *Horizontal strains (%) within grid shown in Figure 21 for the new code – +8% difference to strain gauge data*

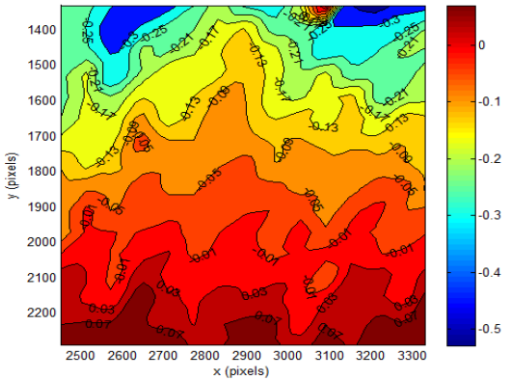

Figure 23: *Horizontal strains (%) within grid shown in Figure 21 for the geotechnical code - +/-14% difference to strain gauge data*

It can be observed that the consistency of the strains across the pixel grid and the magnitude of the %difference between the PIV results and the strain gauge show that the new code is reasonably accurate and far superior to the existing geotechnical code.

3.2.2 Test sample

The CLT ribbed slab test sample was as shown in Figure 24 below.

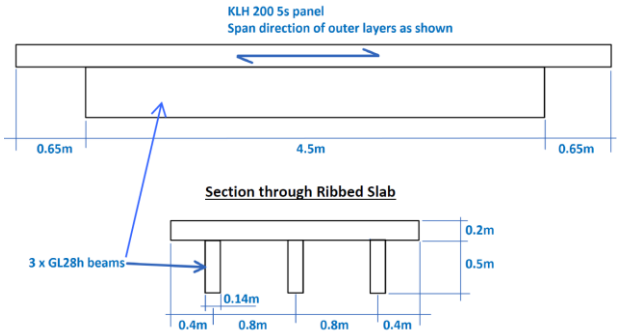

Figure 24: *CLT ribbed slab test sample specification*

Two rows of 5no. 10dia. x 360mm fully threaded screws were also inserted at each rib end at approx. 45mm c/c. Screw details are as per Figure 26 below. The set-up replicated the support condition analysed in the FE modelling described in Section 3.1.3 above.

The sample was tested in 3-point bending for a span of 5.5m, on timber bearers on steel channel sections at each end and the load applied via a steel spreader beam. The experimental set-up is shown in Figure 25 below including the full set of instrumentation installed.

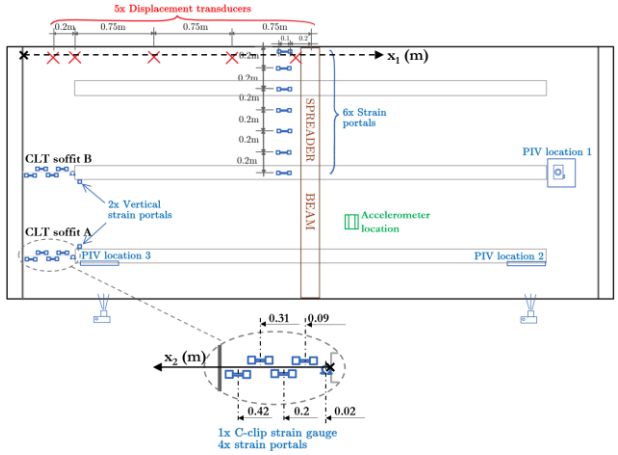

Figure 25: *Test set-up with instrumentation including PIV locations*

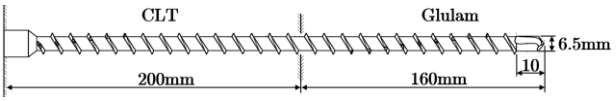

Figure 26: *Fully threaded screw used at the glulam rib cut-back location*

3.2.3 Results

The deflection of the slab was measured via five displacement transducers placed along the span. It was seen that these measurements closely matched the prediction from the FE model whereas the theoretical analysis of the spreadsheet was found to overestimate the deflections (Figure 27 below shows how the 3 methods compare). The overestimation of the theoretical method could be attributed to the conservative effective width used when calculating the stiffness properties.

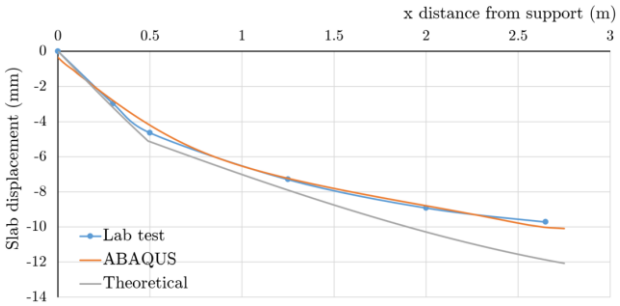

Figure 27: *Deflected shape of top of slab from support to midspan*

Since the stresses perpendicular to the grain, σ_{33}, were of particular interest at the glulam rib end, the vertical strains, ε_{33}, were measured by the PIV method at location 2 and with vertical portal strain gauges fixed to the side of the ribs (refer to Figure 25 for instrumentation locations). One of the portals agreed closely with the PIV method, however, the other had approx. 40% difference.

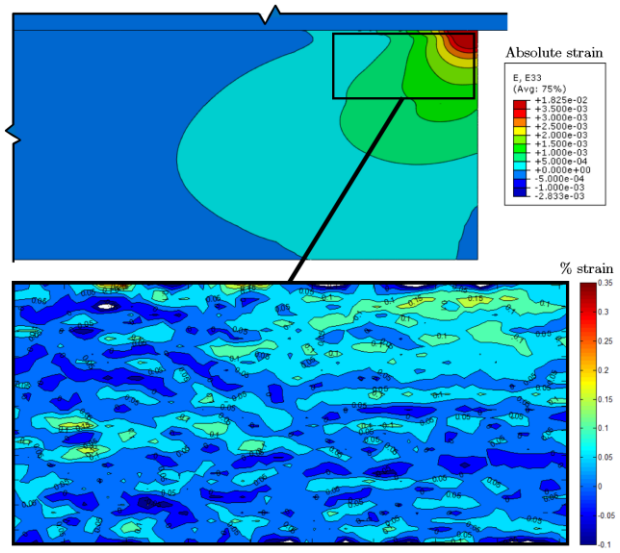

Figure 28: *Vertical strains, ε_{33}, on side of glulam rib, ABAQUS (top), PIV lab test results (bottom)*

Figure 28 above shows the comparison between the vertical strains, ε_{33}, from the FE model and the PIV test results. Although the overall shape of the contours of the PIV results resemble the FE model results, the PIV results appear quite spotty and of lower magnitudes especially at the top right highly stressed corner. The shape of the PIV results can possibly be attributed to the highly anisotropic properties of the wood perpendicular to the grain, including the presence of knots, one of which is apparent centre left in Figure 28.

The low magnitudes of the strains were common to both the PIV results and the strain gauges. After conducting some further literature review, it was suggested that the stiffness of timber perpendicular to the grain is greatest when the growth rings are perpendicular to the stiffness direction [5]. FE modelling of this behaviour illustrates that the stresses in the middle of the growth rings can be twice as high as at 45^0 which is similar to the orientation of the growth rings at the sides of the glulam ribs (see Figure 29). A further consideration why the PIV strains at the corner location are low could be due to the smoothing algorithm in the Matlab code that does not work as well near boundaries. The strain gauge can only provide an average over its length that, in turn, could make it unable to return the high localised corner stresses.

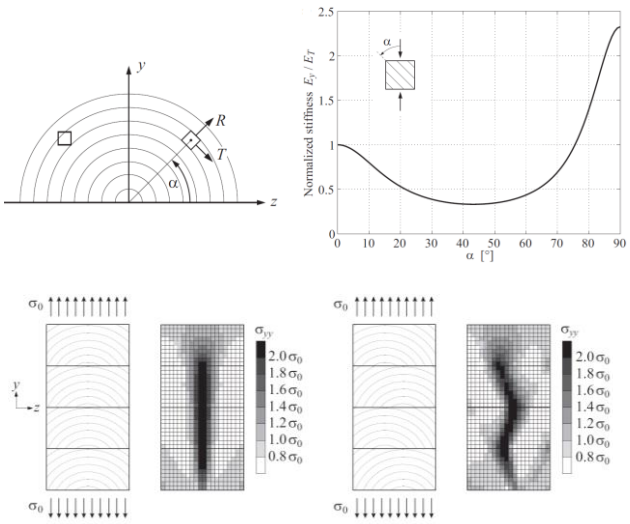

Figure 29: *Stiffness and stress variation of timber dependent on the angle of the growth ring orientation (from Danielsson* **[5]***).*

The fundamental frequency of the test sample was determined using an accelerometer as shown in Figure 25 and by striking the top of the slab with a hammer. The hammer was struck several times and the results were analysed using a Fourier transform in Matlab and averaged. The fundamental frequency from the hammer test was found to be 22.5Hz and from the FE model 25.8Hz. The FE model's stiffer response was thought to originate from the definition of the support conditions as the pinned supports specified were able to restrain the vertical movement both upwards and downwards, whereas during the lab test the slab was simply rested on the supports.

The theoretical calculation using equation (4) gave a natural frequency of 39Hz which is 50% higher than the other 2 methods. The values inserted in the equation were average figures for $(EI)_{\text{eff}}$ and modal mass, m, and this indicates that this might not be applicable to beam elements with variable cross-section. It is thought that the stiffness lost because of the cut-back could be the cause of this overestimation.

3.2.4 Failure mode

As a final test, the sample was load-tested to failure to provide insight as to whether the FE analysis and any observations described in Section 3.1 were accurate.

The test was again a 3-point bend and failure occurred at a total applied load of 236kN by the splitting of 2 glulam ribs at the tips of the screws (see Figure 30 below). This confirmed the expectations that identified that there were high stress concentrations in the timber at the screw tips which were higher than the timber strength perpendicular to the grain.

Figure 30: *Failure mode of CLT ribbed slab test sample by splitting at the screw tips*

Furthermore, it was observed that the CLT slab and the glulam rib debonded at the cut-back corner, which was also identified by the FE model (see Figure 18) as a location of overstress (see Figure 31 below).

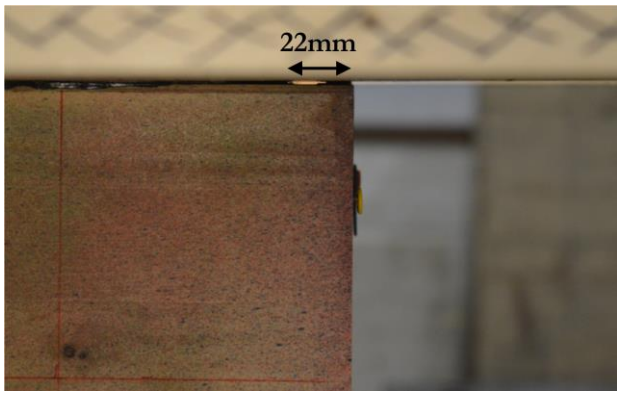

Figure 31: *CLT slab and glulam rib debonding at cut-back corner*

It must be noted that the support reaction at failure nearly matched what was used in the FE analysis (the support reaction at failure in the test was 236/6 = 39.3kN which is very close to the 40kN used in the FE analysis) which means that the glulam splitting occurred at a stress of 4MPa. This is significantly higher than the 0.5MPa proposed by the relevant glulam standard and it is thought that this occurred due to the high stress being over a very small area.

4 THE GPUTC PROJECT

4.1 SPECIFICATION OF CLT RIBBED SLAB

The industrial advisors and sponsors of the research project, Smith and Wallwork consulting engineers, were appointed as the structural designers of a new educational building at Peterborough, UK - the Greater Peterborough University Technical College (GPUTC). The main structural material for the building was CLT and it was completed in August 2015.

A CLT ribbed slab was specified to form the ceiling of a column-free "events space" due to the long-span requirements of 11.5m (see Figure 32 below) and its use as a transfer structure. Similar to the research project, the glulam ribs were stopped short from the supports to allow services to run through and to allow the CLT deck to bear directly on top of a long-span timber truss. It was not possible to adopt a castellated support as this would have taken out most of the truss top chord and if direct shear connections were specified for the end of the ribs, then some of them would clash with the internal steel plate truss connections.

Figure 32: *CLT ribbed slab with cut-back glulam ribs as built in GPUTC*

4.2 LINKS WITH THE RESEARCH PROJECT

The design and installation of the CLT ribbed slab at GPUTC was completed before the research project produced its final results. As observed in the laboratory test and the FE model results, the stress concentrations at the screw tips was the apparent governing failure mode.

This had not been identified at the design stage and the designers undertook additional checks to take this into account in order to confirm that the as-built structure satisfied all structural requirements.

Moreover, an unstressed vibration analysis was run in ABAQUS, replicating the loading scenario of the full 11.5m span. The fundamental frequency obtained was 8.9Hz which is above the general guidance value of 8Hz of Eurocode 5 relevant to residential joisted floors. This gave more confidence in the use of CLT ribbed slabs to meet SLS criteria in such long span scenarios.

5 DESIGN GUIDANCE

The design case with screws partially penetrating into the glulam rib was thought to be similar to the design of notched beams as described in Eurocode 5 since the failure mode of both would be in splitting perpendicular to the grain.

It is suggested that the location of the cut-back with reinforcing screws is designed as a "notional" notch. The research project verifies that any depth of timber within the screw length is adequately reinforced against splitting.

However, the design case described in this project has an increased complexity due to the fact that at the glulam end location there is both a moment and a shear in the CLT slab. As described in Section 3.1.3, this leads to a higher pull-out force to be carried by the screws.

This pull-out force was thought to be the equivalent of a support reaction applied at the face of a notched beam with the penetration depth of the screws into the glulam rib as the effective height, h_{ef}, as noted in the Eurocode design. The effective height stops at the location of the screw tips and introduces the surface where failure will potentially occur. This design scenario is shown in Figure 33 below.

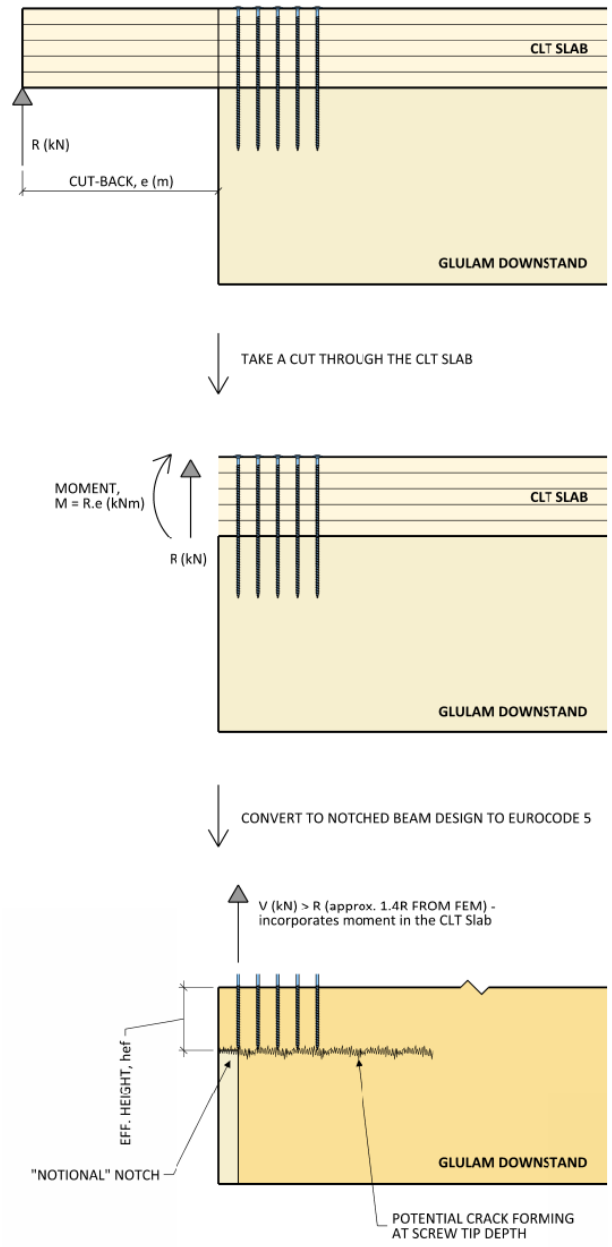

Figure 33: *Glulam rib cut-back location: design case to Eurocode 5 as an equivalent "notional" notch*

The test sample properties were inserted in a notched beam design to check whether this recommendation can yield safe designs. It was found that the "notional" notch design case was conservative by yielding a value of expected capacity 40% smaller than the support reaction at the failure load observed.

Moreover, a taper can be introduced to the glulam rib which, according to the Eurocode design, can have a higher capacity than a 90^0 notch. Using tapered beams as ribs of a CLT ribbed slab is again expected to yield some form of stress concentration at the taper location due to the changing cross-section but it is thought that these should be smaller than with the cut-back rib described in this research project. Eurocode 5 suggests that beams with tapers near the support, where the slope of the taper is more than 1:10, need not be checked for stress concentrations.

6 CONCLUSIONS

It can be concluded that CLT ribbed slabs with cut-back ribs can be used to provide a structural element that can perform well in long spans in terms of deflections and vibrations but require careful detailing at the location where the rib stops.

Finite Element modelling of such systems can provide useful information about their performance. FE analysis performs best when looking at deflection and vibration characteristics and gives useful insight into the stress distribution at the cut-back location. It can be used to identify localised stress concentrations in the timber elements and make a prediction of the failure mode. It is envisaged that more accurate stress distributions can be obtained by increasing the complexity of the material properties to accommodate the anisotropic nature of timber.

Test results confirmed that if the screws only partially penetrate the timber, then the screw tip becomes the most likely location of failure by splitting perpendicular to the grain. It is, therefore, recommended that any reinforcing screws specified are long enough to be able to penetrate as far into the glulam as possible. A baseline value can be taken from BS5268-2, where it is suggested that beams with square notches at the supports should have an effective depth not less than half the depth of the beam.

Vibration results suggested that the generic equation for calculating the fundamental frequency of a system might not be applicable to slabs with variable cross-section and might lead to overestimation.

Concluding, the Particle Image Velocimetry technique was deemed adequate to provide general strain distributions but needs to be refined further to form a consistent source of collecting and analysing data. This method is currently being used and further refined in more research projects at Cambridge University.

REFERENCES

[1] M. Augustin, T. Bogensperger, G. Schickhofer and A. Thiel, "Mitwirkender Breite bei Plattenbalken aus BSH und BSP," 2014.

[2] FP Innovations, CLT Handbook, 2013.

[3] G. Schickhofer, BSPhandbuch, TU Graz, 2010.

[4] N. Niem, CLT composite rib slabs, Cambridge University Engineering Department, 2015.

[5] H. Danielsson, "Perpendicular to grain fracture analysis of wooden structural elements, Models and Applications," 2013.